JOURNAL OF GUIDANCE, CONTROL, AND DYNAMICS
Vol. 27, No. 6, November–December 2004

Efficient Minimax Control Design for Prescribed Parameter Uncertainty

Dirk Tenne* and Tarunraj Singh†
State University of New York at Buffalo, Buffalo, New York 14260

The purview of this paper is the design of a controller that includes knowledge of parametric uncertainties and their distributions. The parameter distributions are approximated by a finite set of points that are calculated by the unscented transformation. This set of points is used to design robust controllers that minimize the worst performance of the plant over the domain of uncertainty. The proposed technique is illustrated on two benchmark problems. The first relates to the design of prefilters for a spring–mass–dashpot system and the second is the feedback control of a hovering helicopter. Numerical simulations are used to illustrate the proximity of the resulting controller to the minimax controller.

Nomenclature

A = system matrix
A_i = amplitudes
B = input matrix
c = damping coefficient
E = energy
f = nonlinear function
f_x = probability density function of x
G = transfer function
h = height
J = cost function
K = control gain
k = stiffness coefficient
m = mass, mean value
n = number of states
P = transition matrix between costates and states
P_x = state covariance matrix
$\mathcal{P}$ = parameter set
$\boldsymbol{p}$ = parameter vector
Q = weighting matrix
R = weighting matrix
s = Laplace variable
T_i = switch times
t = time
u = control input
w = random input, weighting parameter
X = random variable (input)
x = state vector
Y = random variable (output)
y = distance measure
α = significance level
Δ = difference operator
δ = deflection of the longitudinal cyclic stick of the helicopter
ζ = σ point of the input
η = σ point of the output (transformed state)
κ = scaling parameter
μ = central moment
μ_x^i = ith central moment of the random variable x
σ = σ point or set
σ_p = parameter deviation margin
ω = eigenfrequency

Subscripts

f = final
i = counting index
lb = lower boundary
nom = nominal value
p = parameter
res = residual
td = time delay
ub = upper boundary
w = reference to process noise

Received 25 July 2003; revision received 9 March 2004; accepted for publication 11 March 2004.

*Graduate Student, Control, Dynamics, and Estimation Laboratory, Department of Mechanical and Aerospace Engineering. Student Member AIAA.

†Associate Professor, Control, Dynamics, and Estimation Laboratory, Department of Mechanical and Aerospace Engineering.

Introduction

CONTROLLERS are generally synthesized by assuming nominal parameters to represent the plant model. However, the plant parameter can vary during the life cycle due to fatigue, environmental changes, or degrading system components, for example, a leaking damper. The fidelity of such controllers degrades when they are used in such systems. Besides the employment of controllers that detect the changes in the plant (i.e., the theory of adaptive control), research has also been focused on robust control, that is, desensitizing the controller to modeling errors.

Robust control laws describe a set of control parameters that despite varying plant characteristics yield reasonable performance. A controller designed for a nominal plant can perform considerably poorly when the plant characteristics change. Assuming prescribed knowledge of the plant variations, the robust control design identifies the worst operating point of a plant and seeks the optimal set of control parameters for this plant. This tradeoff compromises the controller's performance at the nominal plant with the benefit of satisfactory performance over the anticipated plant variations.

The plant variations are represented in the mathematical model by a set of parameters. For example, the eigenfrequency of a mechanical model can be prescribed to lie in an interval with lower and upper bounds. Doyle[1] and Bryson and Mills[2] defined the parameter deviation interval as a box centered at the nominal plant, where the worst parameter combination has been approximated to lie at the corners of $\mathcal{P}$ (which is true for conservative systems[3]). In real systems, additional information about the bounds of the parameters and their distributions may be available as manufacturer's specifications. This research investigates robust control design including uncertain model parameters, which can be described by their probabilistic distribution, that is, the probability density function (PDF). The relationship between the parameter statistics and the performance index statistics is obtained via the unscented transformation (UT), developed originally for nonlinear filtering by Julier

et al.[4] This method accurately calculates the statistics of a nonlinear transformation up to the second-order moment and, in the case of Gaussianity, up to the fourth-order moment. In contrast to linearization of the nonlinear function, the UT approximates the PDF by a finite number of central moments.

This paper opens with a discussion of capturing the distribution of parametric uncertainties using the UT.[4] This is followed by the conception of a cost function, which results in controllers emulating the minimax controller. The next section illustrates the proposed approach on the design of time-delay filters for rest-to-rest maneuvers of a nonlinear system and a robust feedback controller for a helicopter in hover and concludes with some remarks.

Statistical Robust Controller Design

Consider the first-order mathematical model of a plant:

$$\dot{x} = f(x, p, u) \tag{1}$$

where $x(t) \in \mathcal{R}^n$ is the n-dimensional state and u represents the control input. The uncertain parameter vector $\boldsymbol{p}$ is bounded in the interval space

$$\mathcal{P} : \boldsymbol{p} \in [p_{\text{lb}} \quad p_{\text{ub}}] \tag{2}$$

The lower (p_{lb}) and upper (p_{ub}) limits on the parameters are known quantities, which for example represent mechanical limits such as the stiffness coefficient of a spring. Additional information, however, about the probabilistic distribution of the parameter vector $\boldsymbol{p}$ is often available, which can be described by the joint pdf (probability density function)

$$f_P(p) = \begin{cases} f_P^{\text{in}}(p) & \forall p \in [p_{\text{lb}} \quad p_{\text{ub}}] \\ 0 & \text{elsewhere} \end{cases} \tag{3}$$

where $f_P^{\text{in}}(p)$ is the pdf within the parameter interval. The subsequent text introduces two types of distributions, 1) the uniform distribution and 2) the truncated Gaussian distribution.

Model Parameter Distributions and Approximations

Assuming that the variations of the plant parameters are independent of each other, it is sufficient to describe one-dimensional distributions because the joint pdf is composed of the product of the independent pdfs. If no further knowledge about the parameter variations is available (i.e., every possible plant realization is equally likely), a uniform distribution should be considered, where

$$f_P^{\text{in}}(p) = 1/(p_{\text{ub}} - p_{\text{lb}}) \tag{4}$$

The statistical robust controller approximates the probabilistic distribution by a finite number of central moments. Table 1 shows the first two moments of the uniform distributed parameter, which can be obtained by integrating the pdf of Eq. (3). The first two central moments are called the mean (m_p) and the variance (σ_p^2), which are measures of the expected value and its spread over the parameter probability space, respectively.

Other types of distributions can be incorporated in the design process described in this work. For instance, consider a truncated Gaussian distribution of a parameter that yields a mixed-type distribution. It is assumed that the $2N\sigma$ range equals the interval length ($p_{\text{ub}} - p_{\text{lb}}$) and therefore the mean and variance of the Gaussian distribution can be determined to be

$$m = \frac{p_{\text{lb}} + p_{\text{ub}}}{2}, \qquad \sigma = \frac{p_{\text{ub}} - p_{\text{lb}}}{2N} \tag{5}$$

Table 1 Central moments for different distributions

Central moments	Uniform distribution	Truncated Gaussian distribution
m_p	$\frac{p_{\text{ub}} + p_{\text{lb}}}{2}$	$\frac{p_{\text{ub}} + p_{\text{lb}}}{2}$
σ_p^2	$\frac{(p_{\text{ub}} - p_{\text{lb}})^2}{12}$	Eq. (7)

Furthermore, the tails outside the interval $[p_{\text{ub}} \quad p_{\text{lb}}]$ are lumped into a discrete probability mass function of height $\alpha = P(p \le p_{\text{lb}})$, which is equivalent to half of the probability of p being outside the interval:

$$\alpha = \int_{-\infty}^{p_{\text{lb}}} g(p)\,\mathrm{d}p = \frac{1}{2}\left[\text{erf}\left(\frac{p_{\text{lb}} - m}{\sqrt{2}\sigma}\right) + 1\right] \tag{6}$$

where $g(p)$ represents the pdf of the Gaussian distribution within the interval. By integrating the mixed-type probability distribution, it can be shown that the parameter mean m_p equals the mean of the Gaussian distribution m and the ratio between the parameter variance to the variance of the Gaussian distribution becomes

$$\sigma_p^2 \big/ \sigma^2 = 1 + (N^2 - 1)2\alpha + (p_{\text{lb}} - p_{\text{ub}})g(p_{\text{ub}}) \tag{7}$$

Depending on the $N\sigma$ range used, the influence of the tails becomes less or more important. For instance, if the continuous distribution covers the 3σ range, the tails account for 0.3% of the area of the distribution and are not significant.

Unscented Transformation

The UT is used in this work to describe the probabilistic characteristics of a nonlinear function. Consider a nonlinear transformation of the random variable X with mean $\bar{x}$ and covariance P_x,

$$Y = f(X) \tag{8}$$

where we would like to approximate the statistics of the transformed random variable Y: for example, the mean and variance.

The key feature of the unscented transformation is that it approximates the probability distribution rather than the nonlinear function (for example, by a Taylor series). The UT selects a σ set consisting of $2n + 1$ points, which are perturbations from the mean by a scaled deviation. The deviations σ_i are defined as the columns of the matrix square root of P_x (Ref. 4):

$$\sigma = \pm\sqrt{P_x} \tag{9}$$

The σ set is defined as

$$\zeta_0 = \bar{x} \tag{10}$$

$$\zeta_i = \zeta_0 + \sqrt{(n + \kappa)}\sigma_i \qquad i = 1, \ldots, 2n \tag{11}$$

such that the σ set exhibits the same probabilistic characteristics as the random variable X, and κ is a design variable of the unscented filter. The weighting scheme

$$\bar{\zeta} = \sum_{i=0}^{2n} w_i \zeta_i \tag{12}$$

$$P_\zeta = \sum_{i=0}^{2n} w_i (\zeta_i - \bar{\zeta})(\zeta_i - \bar{\zeta})^T \tag{13}$$

where

$$w_o = \kappa/(n + \kappa), \qquad w_i = 1/2(n + \kappa) \tag{14}$$

has been selected to match the first four central moments of X, that is,

$$\bar{X} = \bar{\zeta}, \qquad P_x = P_\zeta \tag{15}$$

$$\mu_x^3 = \mu_\zeta^3 = 0, \qquad \mu_x^4 = \mu_\zeta^4 \tag{16}$$

which is true for all Gaussian random variables if κ is selected to satisfy the constraint $n + \kappa = 3$.

The σ points are transformed by the nonlinear relationship

$$\eta_i = f(\zeta_i) \qquad i = 1, \ldots, 2n \tag{17}$$

and the estimate of the mean and variance of Y is obtained by the same weighting scheme:

$$\bar{\eta} = \sum_{i=0}^{2n} w_i \eta_i \tag{18}$$

$$P_\eta = \sum_{i=0}^{2n} w_i (\eta_i - \bar{\eta})(\eta_i - \bar{\eta})^T \tag{19}$$

It can be shown by a Taylor-series expansion that the weighted sequences $\bar{\eta}$ and P_η are approximations of the mean and variance of the transformed variable Y. From propagation equation (17), the σ set can be extracted and a Taylor-series expansion is applied such that the weighted sum of Eq. (18) with the definition of the weights [Eq. (14)] can be written as

$$\bar{\eta} = f(\bar{x}) + \frac{1}{2!}\frac{\mathrm{d}^2 f}{\mathrm{d}x^2}\bigg|_{x=\bar{x}} P_x + \frac{1}{4!}\frac{\mathrm{d}^4 f}{\mathrm{d}x^4}\bigg|_{x=\bar{x}} (n+\kappa) P_x^2 \tag{20}$$

which is an exact representation of the mean $\bar{y}$ up to the second order. In the case of a Gaussian distribution of ΔX, where all odd-order moments vanish due to symmetry and the fourth central moment equals three times its variance square, and $n + \kappa = 3$, this approximation is accurate up to the fourth order. However, after a nonlinear transformation the Gaussianity is not preserved and the probability distribution becomes skewed, yielding nonzero odd-order moments. Similar results can be obtained by evaluating the covariance. It is shown by Julier et al.[4] that the covariance approximation agrees with the true covariance up to the second-order terms in the Taylor series.

Statistical Quadratic Performance Index

Optimal control seeks a control input to the system of Eq. (1) that minimizes a certain performance criteria. For a linear quadratic Gaussian (LQG) controller, for example, the performance index is a quadratic integral cost and for a time-delay filter the cost is composed of the energy remaining in the plant. However, to achieve a satisfactory performance over the entire parameter space as discussed in the preceding section, the performance index should be evaluated at the worst combination of all permissible plant parameters. A first approach developed by Doyle[1] leads to the so-called minimax statement:

$$\min_{u} \max_{p \in \mathcal{P}} J(x, p, u) \tag{21}$$

whose solution u minimizes the worst performance in the parameter interval $\mathcal{P}$. The simultaneous maximization and minimization require the identification of the worst parameter combination during the minimization operation, which can be considerably simplified by prescribing a set of plant parameters approximating the worst case. El Ghaoui and Bryson[3] have identified that the maxima appear at the corners of the parameter space $\mathcal{P}$ for conservative systems and near the corners for lightly damped systems.

To ensure that the minimax approach does not eliminate uncertain plant models that might lie at locations other than the corners of the uncertain hypercube, it is necessary to perform an exhaustive search of the uncertain domain. This can be computationally prohibitive. Using the statistics of the cost function over the uncertain parameter space provides an efficient approach for the determination of a robust controller. The proposed technique investigates the statistics of the performance index, which are induced by the uncertain plant parameters—precisely the statistics of the random parameter space.

In contrast to the minimax approach [Eq. (21)], the statistical cost considers the moments (mom) of the quadratic performance index:

$$\min_{u} \operatorname*{mom}_{f_P(p)} J(x, p, u) \tag{22}$$

The robustness is achieved by requiring the mean and the deviation of $J(x, p, u)$ to be minimized. Minimizing the mean m_J endeavors to yield the best performance, and minimizing the deviation σ_J corresponds to reducing the dispersion, which results in robustness. The resulting cost is

$$\operatorname*{mom}_{f_P(p)} J(x, p, u) = m_J + \sigma_J \tag{23}$$

Statistical Time-Delay Controller Design

This section illustrates the statistical design approach on the time-delay controller design based on the paper by Singh and Vadali.[5] The goal is to minimize the vibration at the end of the prespecified maneuver of a single nonlinear mass–dashpot–spring system. The input force is acting on the mass and the spring is modeled as a hardening spring as described by the following nonlinear differential equation:

$$m\ddot{y} + c\dot{y} + k_1 y + k_2 y^3 = u \tag{24}$$

with the following boundary conditions and nominal plant parameters:

$$y(t=0) = \dot{y}(t=0) = 0 \tag{25a}$$

$$y(t=t_f) = 1, \qquad \dot{y}(t=t_f) = 0 \tag{25b}$$

$$m = 1, \qquad c_{\text{nom}} = 0.2, \qquad k_{1\text{nom}} = 1, \qquad k_{2\text{nom}} = 1 \tag{25c}$$

The nonlinear stiffness coefficient and the damping coefficient are subject to variations; hence, the parameter deviation interval $\mathcal{P}$ is identified as follows:

$$0.7 \le k_2 \le 1.3, \qquad 0.1 \le c \le 0.3 \tag{26}$$

The feedforward control is realized as a time delay/input shaper motivated by the posicast controller.[5,6] Figure 1 shows the configuration where the controller transfer function can be written as

$$G_{\text{td}}(s) = A_0 + A_1 e^{-sT_1} + A_2 e^{-sT_2} \tag{27}$$

which will be referred to as a two-time-delay filter. The performance index of the rest-to-rest maneuver is defined as the total energy stored in the system at the end of the maneuver. The so-called residual energy consists of the kinetic energy and a pseudo-potential-energy term which is zero at the boundary conditions:

$$E_{\text{res}} = \sqrt{\tfrac{1}{2}m\dot{y}(t_f)^2 + \tfrac{1}{2}k_1(y(t_f)-1)^2 + \tfrac{1}{4}k_2(y(t_f)-1)^4} \tag{28}$$

The deterministic minimax optimization procedure proposed by Singh[7] solves the following statement:

$$\min_{T_i, A_i} \max_{k,c} E_{\text{res}} \tag{29}$$

It involves an exhaustive search calculating the residual energy over the parameter deviation interval. Furthermore, closed-form solutions of the residual energy and its gradient with respect to the control parameter are utilized to solve the minimax statement of Eq. (29) using the optimization toolbox of MATLAB®. It should be noted that the optimal time-delay filter is only valid for the specified displacement. The filter has to be redesigned for other maneuvers. This is due to the presence of the nonlinearity in the system.

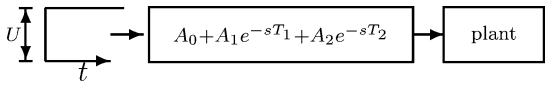

Fig. 1 Time-delay input shaper block diagram.

Plant with Nominal Damping ($c = 0.2$)

Consider the plant operating at the nominal damping value of $c = c_{\text{nom}} = 0.2$. Figure 2 shows the residual energy for three controllers as the nonlinear plant stiffness varies over the uncertain interval. The nonrobust controller (single-time-delay filter) is designed with a constraint that the residual energy be zero for the nominal plant. The sensitivity plot reveals that the energy level increases rapidly as the stiffness deviates from its nominal value. The robust controller (two-time-delay filter) becomes less sensitive to the plant variations and exhibits a 60% decrease of the residual energy at the interval boundaries. The robust controller is designed with the requirement that the residual energy of the nominal plant be constrained to zero. The minimax solution (two-time-delay filter), which eliminates the requirement that the residual energy of the nominal plant be zero, yields a 75% reduction of the residual energy at the boundaries, which becomes a tradeoff as the energy at the nominal plant increases. The largest residual energy in the parameter deviation space, however, is minimized.

The statistical controllers derived with the cost function defined by Eq. (23) are shown in Fig. 3. Assuming a uniform distribution of the stiffness in the parameter deviation space, the statistical controller closely resembles the minimax solution which is designed by discretizing the uncertain space into 10 intervals. On the other hand, while assuming the truncated Gaussian distribution for the nonlinear stiffness, the designer increases the importance of the nominal plant and therefore the residual energy is decreased at the nominal plant. By increasing the σ range of the Gaussian distribution of the stiffness, the residual energy is further decreased at the nominal plant.

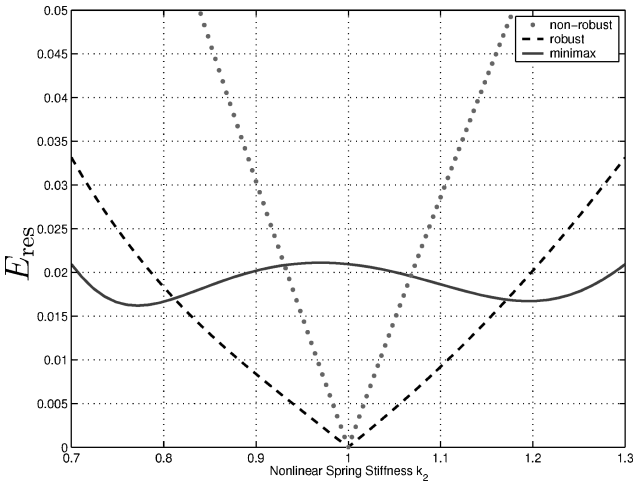

Fig. 2 Residual energy vs plant deviations for standard controller ($c = c_{\text{nom}}$).

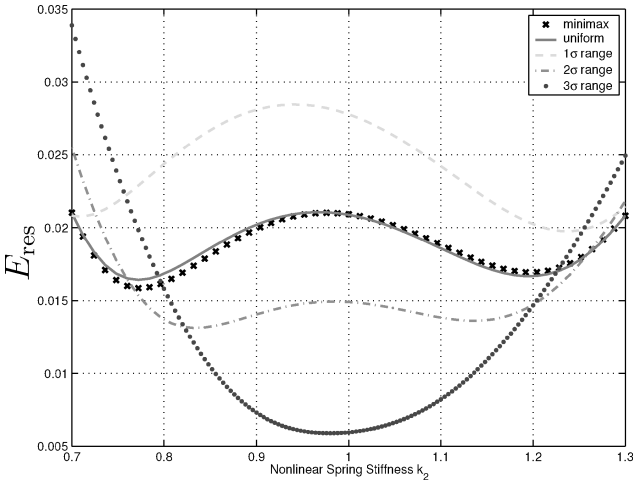

Fig. 3 Residual energy vs plant deviations for the statistical robust controller ($c = c_{\text{nom}}$).

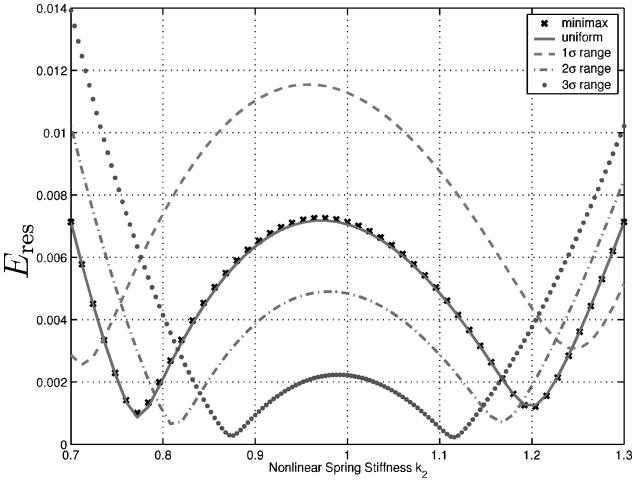

Fig. 4 Residual energy vs plant deviations for the statistical robust controller with three switches ($c = c_{\text{nom}}$).

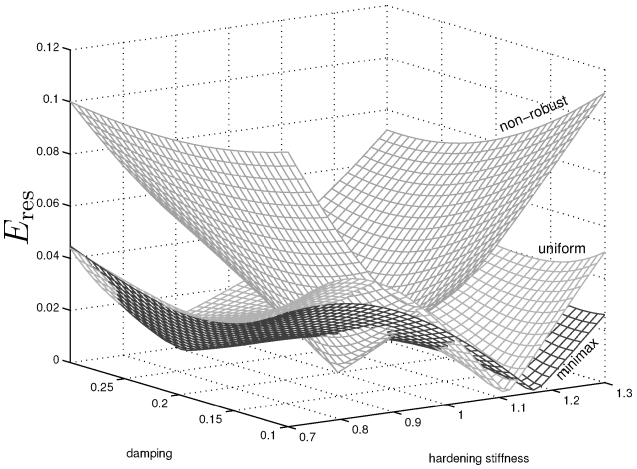

Fig. 5 Residual energy vs plant deviations of the nonlinear stiffness and damping coefficient.

It can be noted from Fig. 3 that the peak at $k_{2\text{nom}}$ shifted to the left as a result of the hardening spring.

The extension to the three-time-delay filter/input shaper yields increased robustness with respect to the nonlinear stiffness variation. Figure 4 shows the residual vibration over possible values of the nonlinear stiffness coefficient. It can be observed that the magnitude of the residual energy is decreased by a factor of 3. Furthermore, increasing the variance of the Gaussian distribution results in the residual energy being reduced in the vicinity of the nominal plant.

Plant with Uncertain Nonlinear Stiffness and Damping

Next, the time-delay controller's robustness is explored assuming uncertainty in the nonlinear stiffness and damping of the plant. Figure 5 shows the behavior of the residual energy as a variation of the plant nonlinear stiffness and damping. The nonrobust time-delay controller excites no vibrations at the end of the maneuver if the plant is operating at its nominal state. Small plant parameter deviations result in large residual vibrations as can be observed from the cone-shaped surface of the residual energy. The minimax solution again yields a superior control profile as the maximum residual energy is minimized over the entire parameter deviation space. The minimax controller design is computationally expensive, which in contrast is significantly reduced by the statistical robust controller. For one optimizer iteration the minimax solver requires 121 function evaluations (if the parameter space is divided into a grid of 11×11 points), whereas the statistical minimization requires $2n + 1 = 5$ σ points to be evaluated. The resulting residual energy surface of the statistical robust controller using uniform parameter distributions

Table 2 Parameters of various time-delay controllers for uncertain plant variation of the nonlinear stiffness and damping coefficient

Time-delay controllers	Time-delay parameters					CPU time
	T_1	T_2	A_0	A_1	A_2	
Standard						
Nonrobust 1 time delay	2.2636	——	0.8587	1.1413	——	196
Robust 2 time delay	2.7893	4.8748	0.5639	0.9639	0.4722	212
Minimax 2 time delay	2.1789	4.9584	0.8450	1.4598	−0.3048	191
Statistic						
Uniform distribution	2.1876	4.9829	0.8431	1.4045	−0.2476	8.77
1σ Truncated Gaussian	2.1909	5.0419	0.8401	1.3961	−0.2363	8.28
2σ Truncated Gaussian	2.1822	4.9393	0.8475	1.4059	−0.2534	7.40
3σ Truncated Gaussian	2.1792	4.9069	0.8501	1.4211	−0.2712	12.47

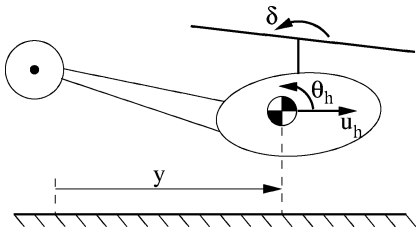

Fig. 6 Hovering helicopter.

approximates the shape of the minimax solution. The residual energy surfaces of the statistical robust controllers for the truncated Gaussian parameter distribution, even though it is not shown in Fig. 5, result in a similar behavior as in the one-parameter case. The truncated Gaussian distribution can be seen as a nonuniform weight on the residual energy cost function resulting in a reduction of the residual energy near the nominal value as the σ range of Eq. (5) increases.

Table 2 lists the time-delay control parameters for the aforementioned controllers. The optimal time-delay controller and the robust two-time-delay controller are derived using the minimax approach. The minimax solution has been obtained by discretizing the parameter space into 11×11 intervals. The last column indicates the computational performance as a measure for comparing the minimax and the statistical controllers. The number of calculations increases geometrically based on the interval size for the minimax approach and arithmetically for the unscented algorithm. The solution of the robust time-delay controller for a linear mass–dashpot–spring system with a nominal spring constant equal to 2 has been used as the initial guess for the optimizers.

Statistical Robust Feedback Controller

Operating a plant at a mode other than the design conditions (the so-called nominal plant) can result in an unstable feedback controller. The uncertainty in the plant is commonly modeled as a set of feedback perturbations illustrating that a minimum degree of stability robustness is guaranteed for the linear quadratic regulator (LQR) subject to phase, gain, and input-multiplicative perturbations.[8] In this section the stability robustness of the LQR as a component within the more general LQG problem is exploited with respect to the probability distribution of the uncertain plant parameters. Considering the example of the hovering helicopter,[2] the UT has been employed to design controllers to increase the stability robustness of the LQR feedback controller.

A hovering helicopter shown in Fig. 6, whose perturbation from a ground point reference is denoted by y and which is subject to wind disturbances u_w, is studied. An optimal robust feedback controller has to be designed minimizing the average distance of the helicopter from the reference point and minimizing the control efforts measured as the deflection of the longitudinal cyclic stick δ, which is proportional to the tilt of the rotor tip-path plane. The cost therefore simplifies under steady-state conditions ($t \to \infty$) to

$$J(p, \delta) = E\{x^T Q x + \delta^T R \delta\} = E\{y^2 + \delta^2\} \tag{30}$$

where the matrices Q and R are the weighting matrices. The quadratic cost is an implicit function of the uncertain plant parameters $p \in \mathcal{P}$ and the control input δ. The decoupled approximation to the longitudinal motion of the OH-6A helicopter can be described by the linear state-space model[2]:

$$\dot{x} = Ax + B\delta + B_w w \tag{31}$$

where the state vector $\boldsymbol{x} = [u_h \;\; q_h \;\; \theta_h \;\; y]$ describes the horizontal velocity u_h, the pitch angle of the fuselage θ_h, and its derivative q_h. The state matrices are given as

$$A = \begin{bmatrix} p_1 & p_2 & -0.322 & 0 \\ p_3 & p_4 & 0 & 0 \\ 0 & 1 & 0 & 0 \\ 1 & 0 & 0 & 0 \end{bmatrix} \tag{32a}$$

$$B = [p_5 \quad p_6 \quad 0 \quad 0]^T \tag{32b}$$

$$B_w = [-p_1 \quad -p_3 \quad 0 \quad 0]^T \tag{32c}$$

where w represents the wind disturbance described as zero mean Gaussian white noise with a variance of $\sigma_w^2 = 18(\text{ft/s})^2$. The six parameters are referred to as the aerodynamic stability derivatives ($p_1, \ldots, p_4$) and as the aerodynamic control derivatives (p_5 and p_6). If the helicopter is operating under design conditions, that is, the nominal plant parameters,

$$p_{\text{nom}} = [-0.0257 \quad 0.013 \quad 1.26 \quad -1.765 \quad 0.086 \quad -7.408] \tag{33}$$

the LQR feedback controller is optimal and is also the solution of the stochastic regulator problem considering the wind disturbances and random initial conditions.[‡] Furthermore, based on the separation principle, the optimal LQG controller consists of an optimal estimator and an optimal LQR part.[8] Minimizing the LQR cost function subject to the state equations requires solving the Riccati matrix equation:

$$0 = -PA - A^T P + P(BR^{-1}B^T)P - Q \tag{34}$$

The optimal feedback gain is defined as

$$u = -Kx = -R^{-1}B^T Px \tag{35}$$

In the case of the hovering helicopter, the feedback gain can be calculated to be

$$K_{\text{LQR}} = [1.9890 \quad -0.2560 \quad -0.7589 \quad 1.0000] \tag{36}$$

and the LQR cost depends on the initial condition $J_{\text{LQR}}(p_{\text{nom}}) = x(0)^T Px(0)$, whereas the value of the cost for the steady-state stochastic regulator (SR) is independent of the initial condition and it can be derived as $J_{\text{SR}}(p_{\text{nom}}) = \text{tr}[PB_w\sigma_w^2 B_w^T] = 1.2194$.[8]

[‡]The cost of the stochastic regulator consists of weighted summands of the LQR cost.

Mills and Bryson[2] have used the Lyapunov matrix equation to derive the cost of the SR. The Lyapunov matrix equation is linear and easier to solve than the Riccati matrix equation, which encounters computational difficulties due to its nonlinearity and stiffness.[9] The cost function of Eq. (30) can be rewritten by using the trace operation and the fact that the control is a state-feedback control:

$$J(p_{\text{nom}}) = tr\left[P_x(Q + K^T R K)\right] \tag{37}$$

The covariance matrix of the state P_x is the solution of the Lyapunov matrix equation, which can be derived by differentiating the expected value of the state-space solution $x(t)x(t)^T$:

$$(A - BK)P_x + P_x(A - BK)^T = -B_w\sigma_w^2 B_w^T \tag{38}$$

Solving the Lyapunov matrix equation and evaluating the cost of Eq. (37) results in the same value as the cost of the stochastic regulator J_{SR} by solving the Riccati equation.

As discussed in the aforementioned text the LQR feedback controller is optimal if the plant is operating at its design specifications and it provides a minimal degree of robustness subject to parameter perturbations. Assume the derivatives of the helicopter system are varying within the set $\mathcal{P}: p \in [p_{\text{lb}} \quad p_{\text{ub}}]$, where the lower and upper interval limits are defined as $0.85p_{\text{nom}}$ and $1.15p_{\text{nom}}$, respectively. As a measure of robustness subject to the parameter deviation, Mills and Bryson[2] introduced the parameter deviation margin σ_p, which corresponds to the normalized parameter deviation such that

$$\frac{p - p_{\text{nom}}}{15\% p_{\text{nom}}} = \sigma_p \tag{39}$$

A value of $\sigma_p = 1/0.15 = 6.667$ would result in an upper bound of zero for the negative parameter and in a lower bound of zero for the positive parameter, which is undesirable because the control derivatives vanish; therefore, the desired parameter deviation is chosen to be $\sigma_p = 6$. For the helicopter parameter this leads to the following parameter interval:

$$p_{\text{ub}} = \begin{bmatrix} -0.0026 \\ 0.0247 \\ 2.394 \\ -0.1765 \\ 0.1634 \\ -0.7408 \end{bmatrix} \qquad p_{\text{lb}} = \begin{bmatrix} -0.0488 \\ 0.0013 \\ 0.126 \\ -3.3535 \\ 0.0086 \\ -14.0752 \end{bmatrix} \tag{40}$$

This parameter space spans a six-dimensional hypercube with $2^6 = 64$ corners. Mills and Bryson[2] formulated the minimax problem assuming that the worst parameter configuration appears at the corners of the hypercube. This minimax technique increased the parameter robustness compared to the LQR solution at the cost of lower performance in the vicinity of nominal plant operation. Figure 7 graphs the inverse of the maximum cost over all 64 corners as a function of the parameter margin deviation σ_p. Increasing the parameter deviation increases the performance index and its inverse approaches zero, which under further increase yields a destabilizing feedback controller. The minimax solution has to be obtained in an iterative procedure because of two factors: 1) the initial guess of the feedback gain that is required to result in a stable closed loop and 2) various local minima of the cost function. The initial feedback gain is obviously taken as the LQR controller gain, which leads to an unstable closed-loop system for the desired parameter margin deviation, $\sigma_p = 6$. The minimax technique iterates the parameter margin starting from a smaller stable σ_p.[2] The second shortcoming is the multi-modal cost function, which requires an iteration of the boundaries of the feedback gain, where initial iterations use tight bounds that are gradually opened to reach the final design. Note that the worst parameter combinations are approximated to lie at the 2^n corners and additional iterations are required to obtain the final minimax feedback gain:

$$K_{\text{minimax}} = [4.2761 \quad -2.2876 \quad -2.8748 \quad 0.4504] \tag{41}$$

The plant parameter perturbations are assumed to be uniformly distributed over the parameter deviation interval such that the PDF constitutes a hypercube of height

$$h = 1 \Big/ \prod_{i=1}^{n} \Delta p_i \tag{42}$$

where $\Delta p_i = p_{\text{ub}} - p_{\text{lb}}$ is the interval of the ith parameter. The PDF can be written using the 15% normalization of the parameter deviation as

$$f_p(p) = \begin{cases} \dfrac{1}{(0.3\sigma_p)^2 \prod_{i=1}^{n} p_{\text{nom}}(i)} & \forall\ p \in [p_{\text{lb}} \quad p_{\text{ub}}] \\ 0 & \text{elsewhere} \end{cases} \tag{43}$$

The UT can be used to approximate the first moments of the parameter space. Subsequently the σ set creates a set of plant realizations with the corresponding set of performance indices. Depending on the choice of the UT, various σ sets can be generated. Figure 8 illustrates the various plant realizations used by the minimax approach and the standard UT, where the first three parameters are varied and the remaining parameters are kept at their nominal values. Figure 8 also includes the cost associated with each plant realization, showing that the worst plant exists at the corner where the parameter perturbations are $[- \quad - \quad +]$. The boxed parameter space creates 2^n plant realizations, whereas the standard UT scales arithmetically ($2n + 1$ plant realizations). As the number of the uncertain parameters increases, the difference between the geometric and arithmetic sequence increases such that for $n = 3$ it is 1 and for $n = 6$ the parameter box has 64 corners and the UT requires 13 plant variations. It can readily be shown that the standard UT with $n + \kappa = 3$ puts the σ set at the parameter boundaries if the parameter PDF is uniformly distributed.

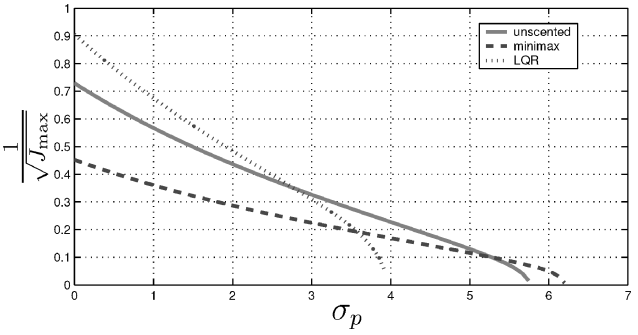

Fig. 7 Maximum cost over all 64 corners vs the parameter margin deviation σ_p.

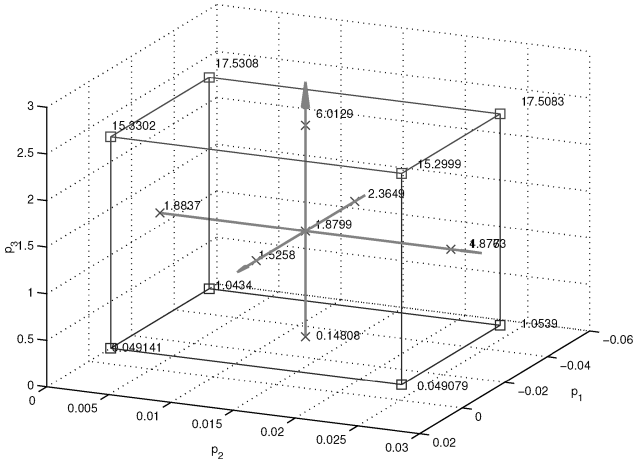

Fig. 8 Parameter deviation space: □, minimax plant realizations; *X*, unscented plant variations, with their respective cost.

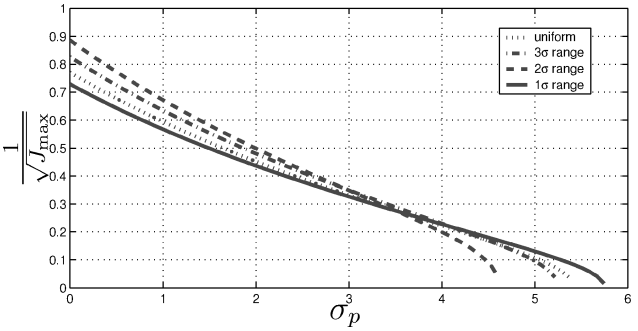

Fig. 9 Maximum cost over all 64 corners vs the parameter margin deviation σ_p as a function of the parameter distribution.

The unscented plant realizations are used to calculate the moments of the cost function of Eq. (30), where the mean resembles the average cost and the variance measures the spread over the parameter deviation. By minimizing statistical cost function (23), we arrive at the statistical robust feedback controller with the feedback gain of

$$K_{\text{unscented}} = [2.4879 \quad -0.6699 \quad -1.8703 \quad 0.9948] \qquad (44)$$

where uniform distribution of the parameters has been assumed. The parameter robustness of the unscented feedback gain is compared to the LQR and minimax feedback gain in Fig. 7. The unscented feedback gain exhibits a perfect tradeoff because the parameter robustness achieved is close to the minimax solution with an overall performance index similar to the optimal LQR cost.

The statistical controller design is amenable to various parameter probability distributions. Figure 9 illustrates the feedback parameter robustness as the parameter PDF is varied from a uniform distribution to three Gaussian distributions. As the σ range increases, the performance at the nominal plant increases and the robustness decreases. On a technical note, the unscented feedback gain has been obtained by utilizing the fmincon routine of the MATLAB optimization toolbox. The initial gain has been the LQR solution of Eq. (36) and the analytical gradient of the cost function has been supplied to the solver. Similar to the minimax approach, some feedback gains result in an unstable closed-loop plant; for example, the initial LQR gain is nonrobust for the desired parameter deviation margin $\sigma_p = 6$. To penalize these feedback gains the optimization problem has been augmented with a nonlinear inequality constraint requiring all closed-loop poles of all plant realizations to lie within the left half-plane. Because the number of plant realizations is small compared to the minimax approach, the number of additional constraints is $(2n+1)n_x = 52$, where the number of parameters is $n = 6$ and the number of eigenvalues is $n_x = 4$. Finally, the sensitivity of the eigenvalues has been provided to aid the optimizer in the search for the constrained minimum, which converges quickly even when starting from an unstable solution.

To evaluate the behavior of the controlled hovering helicopter, the closed-loop poles are studied. Figures 10a to 10c show the closed-loop poles of the 64 corners for a parameter deviation margin σ_p between 0 and 6. It can be seen that the LQR-controlled helicopter becomes unstable for a parameter margin of 3.95 and the unscented feedback controller leads to instability for a parameter margin of 5.6. As seen from Fig. 7, the minimax controller is stable for a parameter margin up to 6.2. Based on this parameter robustness evaluation, it has been observed that the worst plant realization occurs at $[-\ +\ +\ +\ -\ +]$ for the LQR control and at $[-\ -\ +\ +\ -\ +]$ for the minimax and unscented control, where the bracketed expression indicates the corner of the parameter box.

Figure 11 illustrates the variations of the closed-loop poles for the aforementioned worst plant realization. Figure 11 shows the poles of the LQR-controlled helicopter as the parameter margin is increased from 0 to 6. The boldface markers indicate the poles if the helicopter is operating at its nominal values. The overdamped poles on the real axis branch out to oscillating poles and the dominant

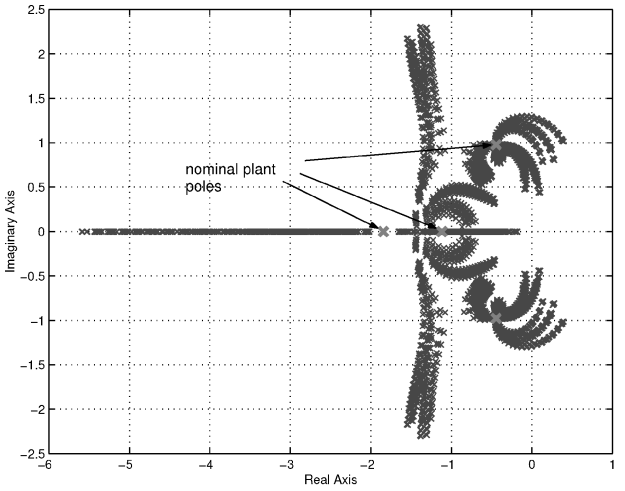

a) LQR-controlled helicopter

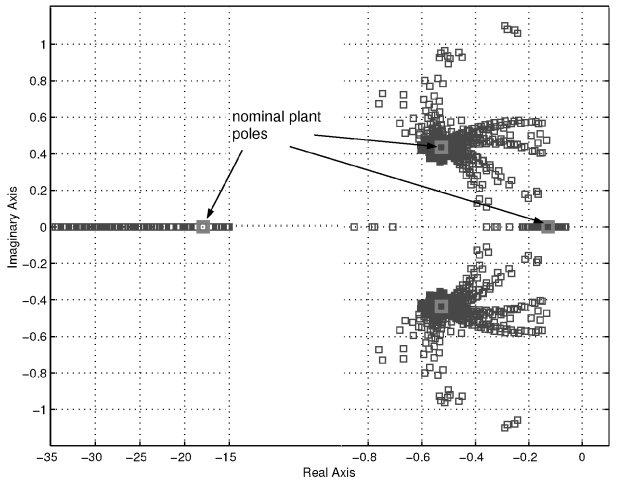

b) Minimax-controlled helicopter

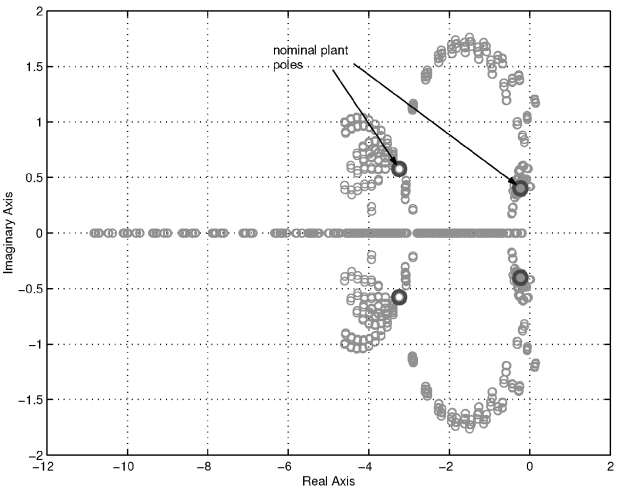

c) Unscented-controlled helicopter

Fig. 10 Closed-loop poles of the 64 corners for increasing parameter deviation margins.

oscillating poles approach the imaginary axis while decreasing the systems damping until the closed-loop plant becomes unstable. The minimax controller places an overdamped pole relatively close to the origin and two poles in the vicinity of the oscillating LQR poles. As the parameter margin increases, the location of the poles are modified by a small amount compared to the changes introduced by the LQR controller. The fourth nonsignificant pole is moving closer to the origin. The unscented controller consists of two oscillating

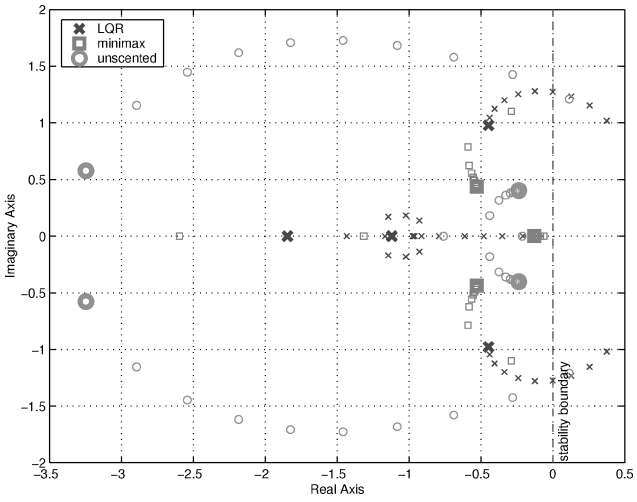

Fig. 11 Worst plant realization closed-loop poles as the parameter margin increases.

pole pairs for the nominal parameters, where one pair is placed in the vicinity of the LQR and minimax controller. As the parameter margin increases, the insignificant pole pair moves toward the imaginary axis increasing the dominance of this pair until further increase results in the system becoming unstable.

Conclusions

The major contribution of this work is a new technique for the design of controllers robust to modeling uncertainties. The domain of uncertainty is assumed to be known as is the distribution of the parameters. The UT is exploited to approximate the distribution of the cost function as a function of the uncertain plant parameters. This leads to a problem formulation that requires a small number of plant realizations to design controllers which closely emulate minimax controllers designed using exhaustive search of the parameter space. Two examples are used to illustrate the proposed technique for the design of prefilters for rest-to-rest maneuver of a vibratory structure and for the design of a feedback regulator for a hovering helicopter, which correspond to nonlinear and linear systems, respectively. Numerical results have shown that the controllers designed by the proposed technique are comparable to the minimax controllers at a fraction of the computation cost.

It should be noted that the efficacy of the proposed technique has only been numerically illustrated on specific cost functions. Because the proposed approach only uses the first two moments of the statistical cost, it is possible that the true minimax solution is not captured for some cost functions.

References

[1]Doyle, J. C., "Analysis of Feedback Systems with Structured Uncertaintly," *IEE Proceedings D, Control Theory and Applications*, Vol. 129, No. 6, 1982, pp. 242–250.

[2]Bryson, A. E., and Mills, R. A., "Linear-Quadratic-Gaussian Controllers with Specified Parameter Robustness," *Journal of Guidance, Control, and Dynamics*, Vol. 21, No. 1, 1998, pp. 11–18.

[3]El Ghaoui, L., and Bryson, A. E., "Worst Case Parameter Changes for Stabilized Conservative Systems," *AIAA Guidance, Navigation, and Control Conference*, Vol. 3, AIAA, Washington, DC, 1991, pp. 1490–1495.

[4]Julier, S. J., Uhlmann, J. K., and Durrant-Whyte, H. F., "New Approach for Filtering Nonlinear Systems," *American Control Conference*, American Automatic Control Council, Dayton, OH, Vol. 3, 1995, pp. 1628–1632.

[5]Singh, T., and Vadali, S. R., "Robust Time-Delay Control," *Journal of Dynamic Systems, Measurement and Control*, Vol. 115, No. 2A, 1993, pp. 303–306.

[6]Smith, O., "Posicast Control of Damped Oscillatory Systems," *Proceedings of the IRE*, Vol. 45, Sept. 1957, pp. 1249–1255.

[7]Singh, T., "Minimax Design of Robust Controllers for Flexible Systems," *Journal of Guidance Control and Dynamics*, Vol. 25, No. 5, 2002, pp. 868–875.

[8]Burl, J. B., *Linear Optimal Control*: $\mathcal{H}_2$ and $\mathcal{H}_\infty$ *Methods*, Addison Wesley Longman, Reading, MA, 1999, pp. 195–230.

[9]Junkins, J. L., and Kim, Y., *Introduction to Dynamics and Control of Flexible Structures*, AIAA Education Series, AIAA, Washington, DC, 1993, pp. 239–249.